The EMBO Journal vol.15 no.21 pp.5824–5832, 1996

Identification of calcium binding sites that regulate potentiation of a neuronal nicotinic acetylcholine receptor

Jean-Luc Galzi[1], Sonia Bertrand[2], Pierre-Jean Corringer, Jean-Pierre Changeux and Daniel Bertrand[2]

URA CNRS D1284, Neurobiologie Moléculaire, Institut Pasteur 75734 Paris Cedex 15, France and [2]Département de Physiologie, Centre Médical Universitaire (Faculté de Médecine), 1211 Geneva 4, Switzerland

[1]Present address: UPR CNRS 9050, Département Récepteurs et Protéines Membranaires, Ecole Supérieure des Biotechnologies 67400 Illkirch, France

The divalent cation calcium potentiates the physiological response of neuronal nicotinic receptors to agonists by enhancing ionic current amplitudes, apparent agonist affinity and cooperativity. Here we show that mutations in several consensus Ca^{2+} binding sequences from the N-terminal domain of the neuronal α7 nicotinic acetylcholine receptor alter Ca^{2+} potentiation of the α7-V201-$5HT_3$ chimera. Mutations E18Q or E44Q abolish calcium-enhanced agonist affinity but preserve the calcium increase of plateau current amplitudes and cooperativity. On the other hand, mutations of amino acids belonging to the 12 amino acid canonical domain (α7 161–172) alter all features of potentiation by enhancing (D163, S169), reducing (E161, S165, Y167) or abolishing (E172) calcium effects on ionic current amplitudes and agonist affinity. Introduction of the α7 161–172 domain in the calcium insensitive 5-hydroxytryptamine ($5HT_3$) serotoninergic receptor results in a receptor activated by 5HT and potentiated by calcium. *In vitro* terbium fluorescence studies with an α7 160–174 peptide further show that mutation E172Q also alters *in vitro* calcium binding. Data are consistent with the occurrence of distinct categories of regulatory calcium binding sites, among which the highly conserved (α7 161–172) domain may simultaneously contribute to calcium and agonist binding.

Keywords: agonist affinity/calcium binding site/ cooperativity/ionic currents/neuronal nicotinic receptors

Introduction

Brain neuronal nicotinic acetylcholine (ACh) receptors are highly permeable to calcium (Mulle *et al.*, 1992a,b; Vernino *et al.*, 1992, 1994; Bertrand *et al.*, 1993; Séguéla *et al.*, 1993). Their responses to agonist are potentiated by calcium ions in a dose-dependent manner (Mulle *et al.*, 1992a; Vernino *et al.*, 1992; Léna and Changeux, 1993; Ramirez-Latorre and Role, 1995). Potentiation by calcium has been shown to occur on native nicotinic receptor species expressed by medial habenula neurons (Mulle *et al.*, 1992a), chromaffin cells (Vernino *et al.*, 1992) and ganglion neurons (Amador and Dani, 1995), as on recombinant receptors composed of *Torpedo* α1βγδ, rat α2β2, α3β2, α3β4, α4β4 and α7 nicotinic receptor subunits reconstituted in *Xenopus* oocytes or fibroblasts (Sine *et al.*, 1990; Vernino *et al.*, 1992; Eiselé *et al.*, 1993; Amador and Dani, 1995; Ramirez-Latorre and Role, 1995).

Several lines of evidence support a physiological modulatory role for calcium on nicotinic receptors. First, synaptic vesicles contain high concentrations of calcium that are released exocytotically from presynaptic neurons, along with the neurotransmitter (Brown *et al.*, 1995). Second, large variations in external calcium concentration have been observed in various brain regions during high synaptic activity (Benninger *et al.*, 1980; Pumain and Heinemann, 1985; Heinemann *et al.*, 1990; Livsey *et al.*, 1990). Third, modulation of the cholinergic spontaneous synaptic currents occurs in ganglionic sympathetic neurons upon rapid changes in external calcium concentration (Amador and Dani, 1995).

On cells expressing nicotinic receptors, calcium ions at millimolar concentration increase whole-cell responses in a voltage-insensitive manner and independently of the presence of calcium chelators injected into the cytoplasm (Sine *et al.*, 1990; Vernino *et al.*, 1992; Eiselé *et al.*, 1993; Amador and Dani, 1995). Furthermore, single-channel recordings reveal that calcium ions increase channel opening frequency (Mulle *et al.*, 1992a; Amador and Dani, 1995) together or not with mean open time (Sine *et al.*, 1990). Moreover, an analysis of the functional α7-V201-$5HT_3$ chimera (Eiselé *et al.*, 1993), containing the N-terminal domain of the chick nicotinic α7 receptor subunit (Couturier *et al.*, 1990) joined to the corresponding C-terminal part of the serotonergic 5-hydroxytryptamine ($5HT_3$) receptor (Maricq *et al.*, 1991), reveals that the chimera, like the α7 nicotinic receptor, is potentiated by Ca^{2+}, whereas the $5HT_3$ receptor is not. These data show that the allosteric effect of calcium ions is mediated by binding sites carried by the N-terminal domain of the nicotinic receptor subunit.

Calcium (II) and the fluorescent lanthanide terbium (III), Tb^{3+}, bind to *Torpedo* nicotinic receptors (Chang and Neumann, 1976; Rübsamen *et al.*, 1976a,b; Fairclough *et al.*, 1986) at sites that resist hydrolysis and are thought to be carried by short polypeptide sequences (Rübsamen *et al.*, 1976a,b, 1978) tentatively assumed to be analogous to those of the metal binding sites present in calcium binding proteins (Persechini *et al.*, 1989; Strynadka and James, 1989; Falke *et al.*, 1994). Such metal sites most frequently exhibit a helix–loop–helix motif, referred to as an EF-hand (Persechini *et al.*, 1989), in which the critical metal binding groups are provided by residues 1, 3, 5, 7, 9 and 12 of a canonical sequence, with a phylogenetically conserved glutamate residue at position 12 (Persechini *et al.*, 1989; Falke *et al.*, 1994).

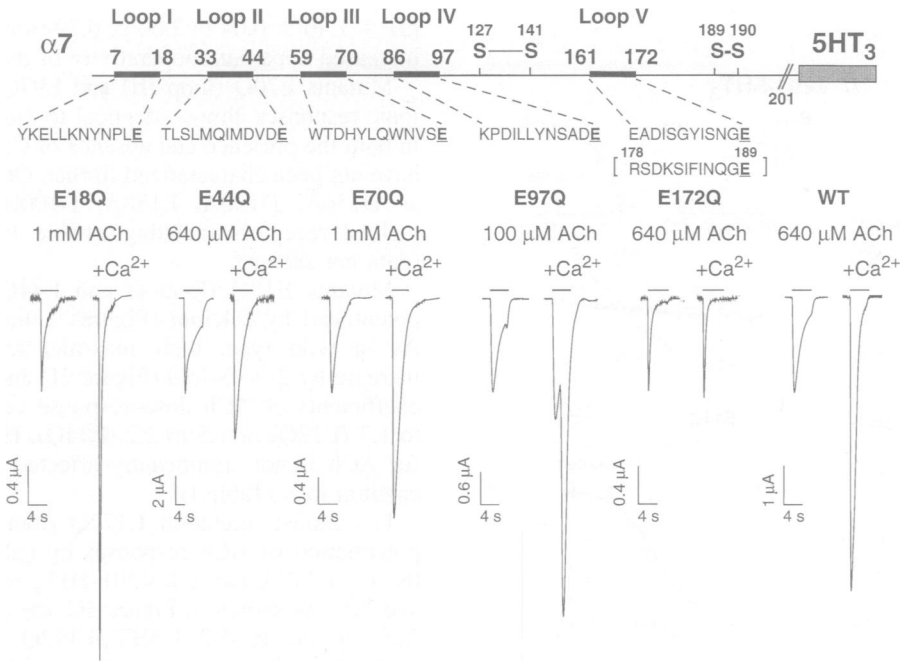

Fig. 1. Upper part: schematic representation of the N-terminal domain of the chick α7 nicotinic receptor subunit depicting the five amino acid sequences detected by the software CALM (Haiech and Sallantin, 1985). These sequences are rich in acidic and hydrophilic groups and contain a terminal glutamate residue. In the α7-V201-$5HT_3$ chimeric subunit shown, amino acids beyond residue 201 correspond to those of the $5HT_3$ receptor sequence. The two disulfide bridges linking Cys127 to Cys141 and Cys189 to Cys190 are shown. The sequence in brackets below the α7 loop V sequence corresponds to that of the $5HT_3$ loop V. Lower part: time course of currents (I_t) evoked by ACh in the absence or presence of 2.5 mM calcium on the α7-V201-$5HT_3$ chimera and its loops *I–V* mutants in which the terminal glutamate residue is mutated to glutamine.

Here, we report that mutations in several putative calcium binding loops from the N-terminal domain of the α7 nicotinic ACh receptor alter calcium potentiation of the α7-V201-$5HT_3$ chimera. Among these loops, domain α7 161–172 exhibits metal binding properties and can be transferred to confer potentiation to the $5HT_3$ receptor. The data further support the occurrence of multiple calcium regulatory sites on nicotinic ACh receptors.

Results

Mutations in the N-terminal domain of the α7-V201-5HT3 chimeric receptor reduce, abolish or increase calcium potentiation

We used the program CALM (Haiech and Sallantin, 1985), designed to search for continuous calcium sites (Haiech and Sallantin, 1985; Strynadka and James, 1989; Falke *et al.*, 1994), to examine the amino acid sequence of the calcium-sensitive nicotinic receptor subunits α1, α2, α3, α4, α7, β1, β2, β4, γ and δ and that of the calcium-insensitive serotonergic $5HT_3$ receptor. We identified five sequences in the N-terminal domain: two of them, located at homologous positions in all subunits tested, correspond to segments 33–44 (loop II) and 161–172 (loop V) of the chick α7 sequence (Figure 1). Loop V ($_{161}$EADISGYIS-NGE$_{172}$) in particular exhibits significant sequence homology with calmodulin calcium site III (DKDGNGYISAAE; Strynadka and James, 1989). Three additional sequences, detected by the software or by visual inspection on only a subset of the subunits and with lower likelihood, correspond to α7 segments 7–18 (loop I), 59–70 (loop III) and 86–97 (loop IV).

Point mutations were introduced in these five sequences at the level of their terminal glutamate residue, namely E18, E44, E70, E97 and E172, to replace them by a glutamine. When analyzed on receptors reconstituted in *Xenopus* oocytes, these mutations had comparable effects on both the chick α7 E237A mutant receptor (Galzi *et al.*, 1992; Bertrand *et al.*, 1993) and the α7-V201-$5HT_3$ chimeric receptor (Eiselé *et al.*, 1993). The mutant α7 E237A was used instead of the wild-type α7 receptor because of its extremely low calcium permeability. However, the low ionic current amplitudes obtained upon expression of this mutant and recorded in the absence of external calcium (Figure 2E and F) prevented a reliable quantitative analysis of the responses. Conversely, the α7-V201-$5HT_3$ receptor can be expressed in large amounts in *Xenopus* oocytes (Figure 1) and HEK 293 cells (Eiselé *et al.*, 1993; Corringer *et al.*, 1995), thus allowing both electrophysiological and equilibrium binding studies to be performed. Therefore the α7-V201-$5HT_3$ receptor was selected as an experimental model and quantitation of the experimental data will be presented only with this chimeric receptor.

In agreement with data reported for native receptors, the potentiation of α7-V201-$5HT_3$ receptor by calcium (Figure 2) occurs in a dose-dependent manner, is stronger at low than at high agonist concentrations (Figure 2B), is not observed if magnesium is added instead of calcium (data not shown) and is insensitive to membrane potential (Figure 2B). An analysis of ACh dose–response curves reveals three effects of 2.5 mM calcium (Figure 2A): (i) the increase in current amplitudes typically ranges from 10-fold at 10 μM ACh to ~2-fold at agonist saturation (Figure 2A and B); (ii) ACh EC_{50} is nearly 3-fold lower (0.0 mM Ca^{2+}, EC_{50} = 67 ± 9 μM; 2.5 mM Ca^{2+}, EC_{50} = 27 ± 9 μM); and (iii) Hill coefficients rise from

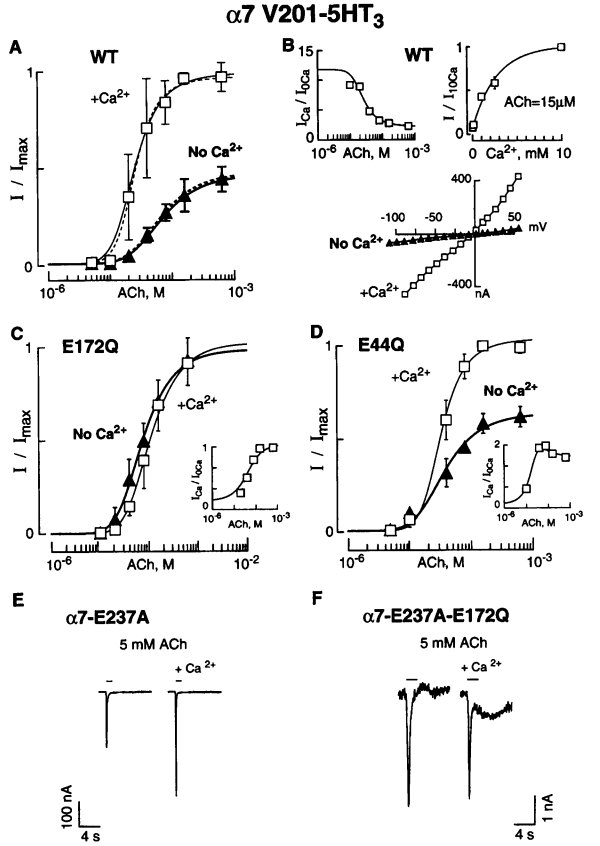

Fig. 2. (**A**) ACh dose–response relationship of the α7-V201-5HT$_3$ receptor in the absence (▲) and presence (□) of 2.5 mM Ca^{2+}. For each cell, data were measured in the two conditions and normalized to the maximal current obtained in the presence of calcium. Data points are the mean ± SD of six cells. Solid lines correspond to fitting with the two-step sequential model (see Materials and methods) with adjusted K and K_0 value ratios, and derived EC_{50} and Hill coefficients, given in Table I. Dashed lines correspond to fitting with the two-state allosteric model (see Materials and methods). (**B**) Upper left panel: plot of the ratio of current amplitudes, measured in the presence or absence of added calcium, as a function of ACh concentration (data points from A). A maximum ratio of ~10-fold is observed at low ACh concentrations, whereas at ACh saturation the ratio is ~2-fold. The solid line corresponds to the ratio of ACh dose–response curve fittings in (A). Upper right panel: plot of agonist-evoked current amplitudes, determined with 15 μM ACh, as a function of external calcium concentration (mean of six cells). Values were normalized with respect to currents evoked at 10 mM Ca^{2+}. The mean current increase between 0 and 10 mM calcium is 13-fold. Lower panel: current–voltage relationship of the α7-V201-5HT$_3$ receptor recorded in the absence (▲) and presence (□) of 2.5 mM Ca^{2+}. Currents were evoked by an ACh concentration near the EC_{50}, and determinations were effectuated after the injection of ~7 mM BAPTA in the oocyte (Galzi *et al.*, 1992). Reversal potentials determined in the absence and presence of calcium are respectively –2 and –3 mV. (**C** and **D**) ACh dose–response relationships of the α7-V201-5HT$_3$ receptor with point mutation E172Q (mean of 10 cells, C) or E44Q (mean of three cells, D) in the absence (▲) and presence (□) of 2.5 mM Ca^{2+}. Solid lines correspond to fitting with the two-step sequential model with adjusted K and K_0 value ratios, and derived EC_{50} and Hill coefficients, given in Table I. Insets represent the current ratios obtained (as in Figure 1B) as a function of the ACh concentration. (**E** and **F**) Time course of currents (I_t) evoked by ACh in the absence or presence of 2.5 mM calcium on the α7 E237A receptor mutant and its α7 E237A-E172Q mutant, in which the terminal loop V glutamate residue is mutated to glutamine. The very small amplitude of the double mutant prevents reliable measurements over a broad ACh concentration range. The slow current fluctuation is attributable to solution exchange artifacts.

nH = 1.40 ± 0.04 to 2.00 ± 0.29 (see Table I), reflecting increased apparent cooperativity of the response.

Mutants E70Q (loop III) and E97Q (loop IV) display ionic responses almost identical to those of the wild type in both the presence and absence of Ca^{2+} (Figure 1); they have not been characterized further. Other mutations, such as D156A, D130A, E188A, D100H and D88A, also yielded receptors indistinguishable from the wild type (data not shown).

Mutants E18Q (loop I) and E44Q (loop II) remain potentiated by calcium (Figures 1 and 2D and Table I). As in wild type, their maximal response amplitudes increase by 2- to 3-fold (Figure 2D and Table I), and Hill coefficients of ACh dose–response curves rise from 1.3 to 1.7 (E18Q) or 1.5 to 2.2 (E44Q). However, their EC_{50} for ACh is not significantly affected by the addition of calcium ions (Table I).

In contrast, mutation E172Q (loop V) abolishes the potentiation of ACh responses by calcium ions on both the α7 E237A and α7-V201-5HT$_3$ receptors (Figures 1 and 2F). As shown in Figure 2C, the addition of 2.5 mM Ca^{2+} to the α7-V201-5HT$_3$-E172Q receptor results in negligible changes in response amplitudes, apparent affinity for ACh ($EC_{50}[0.0Ca^{2+}]$ = 78 ± 16 μM; $EC_{50}[2.5Ca^{2+}]$ = 111 ± 18 μM) and cooperativity of the response ($nH_{[0.0Ca^{2+}]}$ = 1.4; $nH_{[2.5Ca^{2+}]}$ = 1.4). Moreover, these EC_{50} values and Hill coefficients are almost identical to those determined in the absence of calcium on the wild-type receptor (Table I). Thus mutation E172Q abolishes calcium potentiation without significantly altering the other parameters of the response to ACh.

Binding of ACh, measured as the inhibition of [^{125}I]α-bungarotoxin (α-Bgtx) binding (Weber and Changeux, 1974; Corringer *et al.*, 1995), reveals that upon adding 10 mM calcium, the ACh apparent dissociation constant (K_p values in Table II) weakly decreases for the α7-V201-5HT$_3$ receptor or weakly increases for the E172Q mutant. Binding measurements performed on E18Q and E44Q mutants reveal no significant differences between 0.0 and 10 mM calcium.

Because the most critical mutant, E172Q, belongs to loop V, we systematically mutated residues E161, D163, S165, Y167 and S169 which respectively occupy consensus positions 1, 3, 5, 7 and 9 of a putative calcium binding loop. Mutants E161R, S165E, Y167F and S169E exhibit, in the absence of external calcium ions, EC_{50} values and Hill coefficients comparable with those of the wild type (see Table I). At variance, as described for *Torpedo* receptor (Czajkowski *et al.*, 1993), mutation D163N reduces the apparent ACh affinity. In all cases, however, potentiation is maintained, as indicated by the concomitant increase in apparent ACh affinity, cooperativity and maximal response amplitude (Table I) upon adding 2.5 mM calcium. An increase of apparent affinity and maximal response amplitude (Table I) is significantly more pronounced for mutants D163N and S169E; it is less pronounced for mutants E161R, S165E and Y167F than for wild type. Therefore, several mutations at different positions within loop V interfere with calcium potentiation.

Potentiation of the 5HT$_3$ receptor upon transfer of the α7 161–172 domain

Transfer of α7 loop V into the wild-type 5HT$_3$ receptor was used as an additional test for its contribution to

Table I. Electrophysiological properties of the effects of external calcium on the α7-V201-5HT$_3$ and 5HT$_3$ receptors and their mutants

cDNA type	0.0 mM Ca^{2+}			2.5 mM Ca^{2+}			$EC_{50}[0.0Ca^{2+}]$	$I_{max}[2.5Ca^{2+}]$	$K[0.0Ca^{2+}]$	$K_0[0.0Ca^{2+}]$
	EC_{50} (μM)	n_H	I_{max} (μA)	EC_{50} (μM)	n_H	I_{max} (μA)	$EC_{50}[2.5Ca^{2+}]$	$I_{max}[0.0Ca^{2+}]$	$K[2.5Ca^{2+}]$	$K_0[2.5Ca^{2+}]$
α7-201-5HT$_3$										
Wild type	67 ± 9	1.40 ± 0.04	4.97 (n = 6)	27 ± 9	2.00 ± 0.29	11.18 (n = 6)	2.60 ± 0.59	2.29 ± 0.32	1	12 ± 5
Loop I										
E18Q	13 ± 1	1.30 ± 0.03	2.49 (n = 4)	19 ± 1	1.70 ± 0.20	6.43 (n = 4)	0.68 ± 0.05	2.38 ± 0.67	0.33 ± 0.10	11 ± 7
Loop II										
E44Q	38 ± 11	1.50 ± 0.04	4.38 (n = 5)	32 ± 7	2.20 ± 0.15	7.06 (n = 5)	1.26 ± 0.52	1.65 ± 0.15	0.61 ± 0.45	10 ± 5
Loop V										
E161R	45 ± 6	1.40 ± 0.05	1.03 (n = 5)	27 ± 6	1.90 ± 0.30	2.00 (n = 5)	1.74 ± 0.31	1.93 ± 0.18	1	4 ± 1
D163N	569 ± 25	1.40 ± 0.02	2.12 (n = 4)	156 ± 11	2.30 ± 0.01	7.90 (n = 4)	3.65 ± 0.32	3.82 ± 0.66	1	31 ± 9
S165E	151 ± 21	1.40 ± 0.05	1.42 (n = 8)	73 ± 8	1.80 ± 0.14	2.91 (n = 8)	2.10 ± 0.52	2.16 ± 0.55	1	8 ± 6
Y167F	33 ± 5	1.60 ± 0.06	2.65 (n = 6)	17 ± 3	2.00 ± 0.13	4.62 (n = 6)	1.88 ± 0.05	1.84 ± 0.51	1	4
S169E	123 ± 13	1.40 ± 0.04	1.64 (n = 6)	40 ± 10	2.10 ± 0.03	5.14 (n = 6)	3.22 ± 0.52	3.34 ± 0.54	1	23 ± 7
E172Q	78 ± 16	1.40 ± 0.02	0.91 (n = 16)	111 ± 18	1.40 ± 0.06	0.72 (n = 16)	0.72 ± 0.20	0.88 ± 0.21	0.69 ± 0.20	1.0 ± 0.6
5HT$_3$										
Wild type	3.0 ± 0.5	1.80 ± 0.23	0.98 (n = 8)	3 ± 1	1.90 ± 0.23	0.43 (n = 8)	0.96 ± 0.08	0.38 ± 0.09	0.96 ± 0.10	1
CA1$_{\alpha7\ 161-172}$	23 ± 5	1.40 ± 0.01	2.66 (n = 10)	23 ± 4	2.10 ± 0.07	4.55 (n = 10)	0.98 ± 0.08	1.75 ± 0.39	0.43 ± 0.03	7.0 ± 0.1
CA2$_{\alpha7\ 161-171,172Q}$	7.0 ± 0.5	1.50 ± 0.02	2.23 (n = 4)	17 ± 3	2.00 ± 0.30	3.48 (n = 4)	0.43 ± 0.09	1.40 ± 0.53	0.31 ± 0.05	2 ± 1

All parameters are determined as described in Materials and methods. EC_{50} and n_H values are given for ACh (α7-V201-5HT$_3$) or serotonin (5HT$_3$ receptor).

Table II. Summary of ACh equilibrium binding experiments in the absence and presence of calcium

cDNA type	0.0 mM Ca^{2+}		10.0 mM Ca^{2+}	
	K_p (μM)	n_H	K_p (μM)	n_H
α7-201-5HT$_3$				
Wild type	131 ± 8	1.4 ± 0.1	111 ± 13	1.6 ± 0.1
Loop I				
E18Q	35 ± 13	1.3 ± 0.1	35 ± 4	1.4 ± 0.1
Loop II				
E44Q	451 ± 49	1.1 ± 0.1	510 ± 60	1.0 ± 0.1
Loop V				
D163A	1110 ± 19	1.1 ± 0.1	853 ± 17	1.0 ± 0.1
E172Q	107 ± 11	1.5 ± 0.1	162 ± 4	1.4 ± 0.1

The inhibition of initial [^{125}I]α-Bgtx binding velocity to intact HEK 293 cells expressing the α7-V201-5HT$_3$ and mutated receptors was measured as a function of the ACh concentration in the absence or presence of 10.0 mM Ca^{2+}. K_p and n_H values were determined as described in Corringer *et al.* (1995).

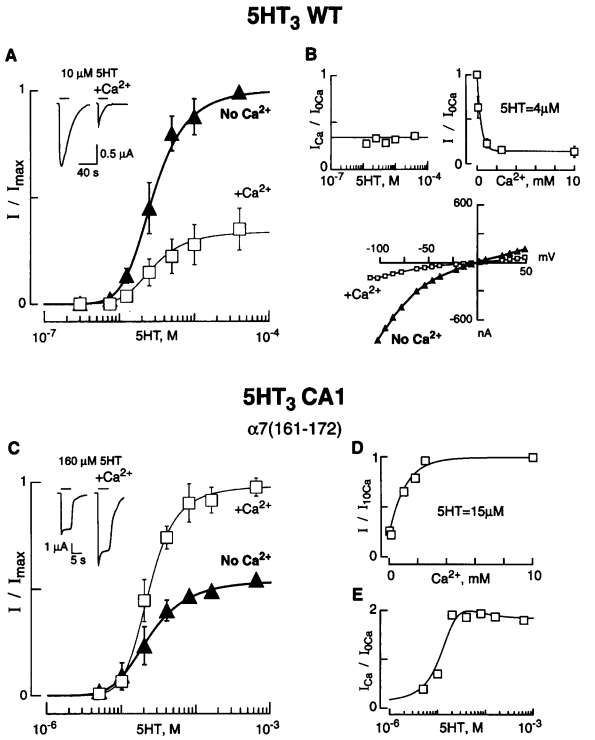

Fig. 3. (**A**) 5HT dose–response relationship of the wild-type 5HT$_3$ receptor in the absence (▲) and presence (□) of 2.5 mM Ca^{2+}. Data points are the mean ± SD of five cells. Solid lines correspond to fitting with the two-step sequential model (see Materials and methods) with adjusted K and K_0 value ratios, and derived EC_{50} and Hill coefficients, given in Table I. Typical time courses of the evoked currents recorded in the two conditions are illustrated in the inset. (**B**) Upper left panel: plot of the ratio of current amplitudes measured in the presence or absence of added calcium as a function of 5HT concentration (data point from A). Each point represents the mean of five determinations. The solid line is the ratio of 5HT dose–response curve fittings in (A). Upper right panel: plot of agonist-evoked current amplitudes, determined with 4 μM 5HT, as a function of external calcium concentration (mean of four cells) The mean current decrease between 0 and 10 mM calcium is 9-fold. Values were normalized to the zero Ca^{2+} condition. Lower panel: current–voltage relationship of 5HT-evoked responses on the 5HT$_3$ receptor in the absence (▲) and presence (□) of 2.5 mM Ca^{2+}. Reversal potentials (–1 mV), determined in the absence and presence of calcium, were indistinguishable. (**C**) 5HT dose–response relationship of the chimeric 5HT$_3$ CA1 receptor obtained in the absence (▲) and presence (□) of 2.5 mM Ca^{2+}. This chimera exhibits the 5HT$_3$ receptor sequence except for residues 161–172 (loop V in Figure 1), which are those of the α7 nicotinic receptor subunit. Data points are the mean ± SD of four cells. Solid lines correspond to fitting with the two-step sequential model with adjusted K and K_0 value ratios, and derived EC_{50} and Hill coefficients, given in Table I. Time course of 5HT-evoked currents recorded in the absence and presence of Ca^{2+} are illustrated in the inset. (**D**) Currents evoked by 15 μM 5HT depend on the external calcium concentration. Currents were normalized with respect to the maximal value determined at 10 mM Ca^{2+}. The current increases as much as 3.5-fold between 0.0 and 10 mM calcium. (**E**) Plot of the ratio of current amplitudes measured in the presence or absence of added calcium as a function of 5HT concentration (data points from C). The solid line is the ratio of 5HT dose–response curve fittings from (C).

calcium potentiation. As shown on Figure 3A and B, responses of the wild-type 5HT$_3$ receptor to serotonin (5HT) decrease upon adding calcium (2.5 mM) in a voltage-sensitive manner (Figure 3B) and without affecting apparent 5HT affinity or Hill coefficients (Table I), as expected if calcium behaves as a channel blocker (Maricq *et al.*, 1991; Eiselé *et al.*, 1993). Introduction of the α7 loop V at the homologous position in the 5HT$_3$ receptor gives the 5HT$_3$ CA1 mutant (Figure 3C–E). In the absence of calcium, this mutant exhibits a lower affinity for 5HT (EC_{50} mutant = 23 ± 5 μM; EC_{50} wild type = 3.0 ± 0.5 μM) and significantly lower cooperativity (n_H mutant = 1.4; n_H wild type = 1.8) than wild type (Table I). Second, calcium increases both response amplitudes at high agonist concentrations and the cooperativity of the response (Figure 3C and Table I), indicating that potentiation takes place. Third, the addition of calcium is not accompanied by alterations of 5HT apparent affinity (0.0Ca^{2+}, EC_{50} = 23 ± 5 μM; 2.5Ca^{2+}, EC_{50} = 23 ± 4 μM; Table I). Fourth, the introduction of a mutation homologous to α7 E172Q in the 5HT$_3$ CA1 mutant (mutation E189Q yielding mutant 5HT$_3$ CA2) almost abolishes potentiation by calcium (Figure 4A–C), supporting a similar functional role for this glutamate residue on both the nicotinic and serotonergic chimeric receptors. Furthermore, two additional microchimeric 5HT$_3$ receptors, in which only half of α7 loop V is introduced (residues 161–166 and 167–172), respond to agonist application. Yet, in the presence of calcium their ionic currents decrease (Figure 4D), as on the wild-type 5HT$_3$ receptor which is not potentiated, indicating that only the complete α7 loop V sequence confers calcium potentiation onto the 5HT$_3$ receptor, and supporting the fact that there are potentiation determinants in each half of that loop.

Metal binding to the α7 161–172 domain

Terbium ions replace calcium in most metal binding proteins/peptides (Rübsamen *et al.*, 1976a,b; McManus *et al.*, 1990; D'Souza *et al.*, 1994), and Tb^{3+}–protein complexes can be detected by fluorescence resonance energy transfer from these sites. The synthetic peptide α7 160–174, which comprises a full loop V, contains two aromatic residues (Tyr167 and Trp173) that can serve as fluorescence energy donors for *in vitro* titration experiments. When Tb^{3+} at a fixed concentration (10 μM) is mixed with increasing amounts of peptide α7 160–174, Tb^{3+} fluorescence is enhanced (Figure 5A). It reaches a

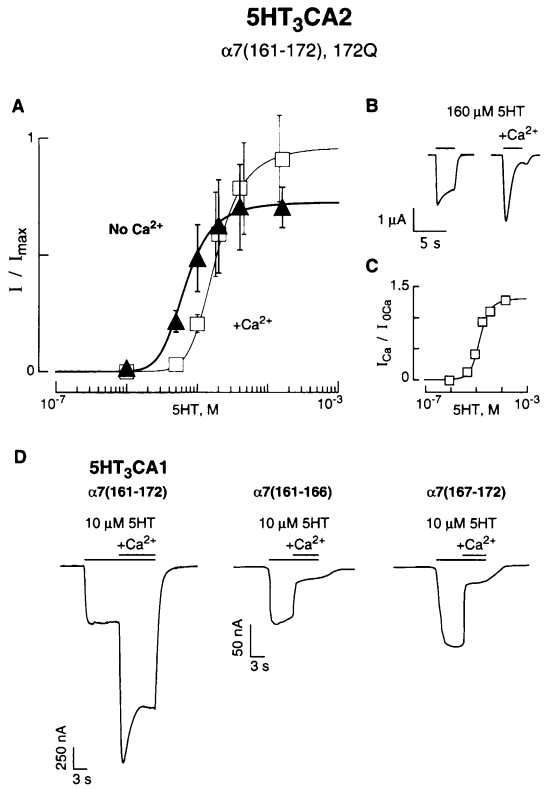

Fig. 4. (**A**) Dose–response relationship of the chimeric $5HT_3$ CA2 receptor to 5HT recorded in the absence (▲) and presence (□) of 2.5 mM Ca^{2+}. This chimera exhibits the $5HT_3$ receptor sequence except for residues 161–171 (loop V in Figure 1), which are those of the α7 nicotinic receptor subunit, and residue E172 mutated to glutamine. Data points are the mean ± SD of four cells. Solid lines correspond to fitting with the two-step sequential model with adjusted K and K_0 value ratios, and derived EC_{50} and Hill coefficients, given in Table I. (**B**) $5HT_3$ CA2 mutant receptor ionic responses elicited by 5HT applications in the absence and presence of 2.5 mM calcium. (**C**) Plot of the ratio of current amplitudes measured in the presence or absence of added 2.5 mM calcium as a function of 5HT concentration (data point from A). The solid line is the ratio of 5HT dose–response curve fittings in (A). (**D**) Ionic responses to 5HT application on oocytes expressing the $5HT_3$ CA1 mutant containing the α7 loop V sequence (residues 161–172) and the two microchimeras containing only part of the α7 loop V (residues 161–166, middle, or residues 167–172, right). Agonist-evoked ionic current is enhanced in the mutant $5HT_3$ CA1 in response to a 0.0–2.5 mM Ca^{2+} jump, whereas it is depressed in the two microchimeric constructs containing only part of loop V.

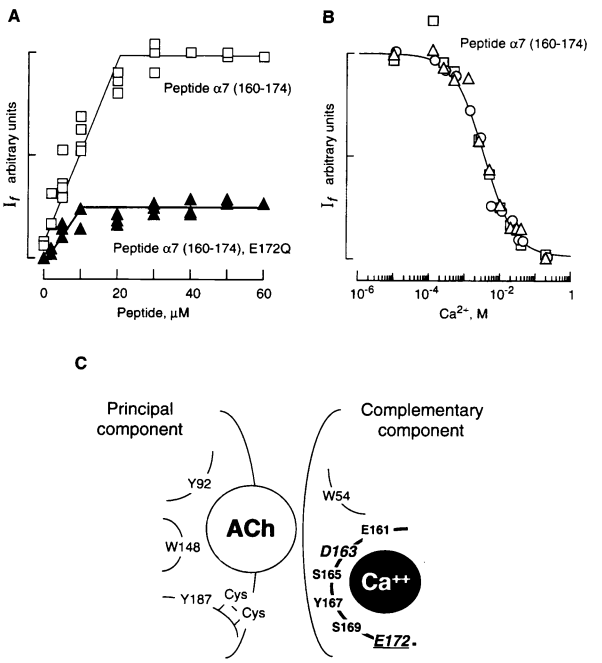

Fig. 5. (**A**) Terbium binding to the synthetic peptide comprising α7 amino acids 160–174 (□) or to the same peptide with the E172Q mutation (▲). Terbium is used at a 10 μM concentration. Data points correspond to four (□) and three (▲) independent determinations. (**B**) Inhibition of terbium (10 μM) binding to 10 μM synthetic α7 160–174 peptide by calcium. The experimental IC_{50} mean value is 3.1 ± 0.4 mM. (**C**) Model of the ACh and calcium binding sites on the nicotinic receptor. Amino acids Y92, W148, Y187, C189 and C190 from the principal component and residues W54 and D163 (α7 subunit numbering) from the complementary component of the ACh binding site belong to five loops (Corringer *et al.*, 1995; Czajkowski and Karlin, 1995; Karlin and Akabas, 1995). The mutation of residues E161, D163, S165, Y167, S169 and E172 (loop V in Figure 1) alters calcium potentiation.

plateau at a peptide:ion ratio of ~1.5–2.0:1, indicating interaction between the peptide and the ion. Moreover, calcium in the millimolar range inhibits energy transfer to Tb^{3+} (Figure 5B), and the substitution of Glu172 by glutamine in the synthetic peptide results in a dramatic reduction of energy transfer (Figure 5A). These data are consistent with the notion that, on the intact receptor, calcium interacts with loop V (Figure 5C) to potentiate the ACh response.

Discussion

The neurotransmitter-gated channels, such as the nicotinic ACh, $5HT_3$, glycine or $GABA_A$ receptors, contain several categories of topographically distinct regulatory sites which differentially recognize agonists, competitive and noncompetitive antagonists, and a large variety of ions, chemicals and peptides as positive or negative allosteric effectors (Léna and Changeux, 1993; Galzi and Changeux, 1994; McDonald and Olsen, 1994; Smart *et al.*, 1994).

Among these effectors, the divalent cations zinc or calcium have been detected in the brain at the level of nerve terminals (Assaf and Chung, 1984; Brown *et al.*, 1995). Zinc ions, for instance, modulate the responses of $GABA_A$ (Draghun *et al.*, 1990; Smart *et al.*, 1994) and glycine (Laube *et al.*, 1995) receptors to their neurotransmitter. In addition, calcium ions bind to several sites on nicotinic receptors (Chang and Neumann, 1976; Rübsamen *et al.*, 1976a,b, 1978; Fairclough *et al.*, 1986) and exert distinct effects on channel properties (Mulle *et al.*, 1992b; Vernino *et al.*, 1994; Amador and Dani, 1995) or on the regulation of channel activation (Mulle *et al.*, 1992a; Vernino *et al.*, 1992; Eiselé *et al.*, 1993; Amador and Dani, 1995) and desensitization (Cohen *et al.*, 1974; Heidmann and Changeux, 1979).

Our work suggests that the calcium effect referred to as potentiation (reviewed in Léna and Changeux, 1993) might itself be mediated by multiple allosteric sites, some of which affect neurotransmitter binding. In agreement with these notions, dose–response curves reveal distinct effects of calcium depending on which residue is mutated from the extracellular domain of the α7 subunit. When

mutations are performed within loop V, analyses of dose–response curves in terms of either a sequential model for channel activation (Del Castillo and Katz, 1957) or a two-state allosteric scheme (Monod *et al.*, 1965; see Materials and methods), are consistent with the assumption that calcium affects solely the isomerization between the resting and open channel states ($K_0 = \alpha/\beta$ in the sequential model or L = [resting state]/[open channel state] in the allosteric model). This interpretation accounts for (i) the calcium-dependent potentiation; (ii) the increased current amplitude at all ACh concentrations, including saturation; (iii) the increased cooperativity of ACh dose–response relationships; and (iv) the calcium-promoted shifts of EC_{50} values. For none of these constructs need the intrinsic affinity of the agonist for its sites be changed by >1.4-fold (see Table I). Similarly, for mutants E18Q (loop I) and E44Q (loop II), analyses of dose–response curves are also consistent with the assumption that calcium affects the isomerization constant (K_0 or L) for channel activation, because these receptors exhibit increased current amplitudes and cooperativities in the presence of calcium. However, the expected change in EC_{50} values is not observed, indicating that calcium may, in addition, alter the intrinsic agonist dissociation constants K (see Materials and methods).

In vitro interactions of Tb^{3+}/Ca^{2+} ions with a peptide (α7 160–174) exhibiting the α7 loop V sequence, together with the fact that loop V confers calcium potentiation to the $5HT_3$ receptor, suggest that residues from the 161–172 segment contribute directly to calcium binding. Yet, within this segment, different mutations at a given position, such as mutations E161-I, -R or -Q, but also D163 -A or -N and S165-E or -K, alter potentiation in a comparable manner (data not shown), suggesting that the chemical nature of the amino acid side chain at these positions is not critical. Thus, at variance with canonical high-affinity calcium sites, all amino acid side chains tested may not point towards the bound calcium ion. As in several low-affinity calcium sites (Falke *et al.*, 1994), they may either not contribute to binding at all, or interact with the metal ion through their backbone carbonyl groups.

Furthermore, the mutation of some residues within loop V, in particular mutations D163N (Table I) and D163A (Table II), together enhance potentiation by calcium and drastically reduce its apparent affinity for ACh in equilibrium binding experiments, suggesting that residue Asp163 may simultaneously belong to a calcium binding loop and to the cholinergic ligand binding area. Several lines of experimental evidence support this view. On *Torpedo* nicotinic receptor, the 9 Å-long affinity cross-linking reagent *S*-(2-[^{3}H]glycylamidoethyl)dithio-2-pyridine establishes a covalent bond between the amino acid Cys192 or Cys193 from the principal component of the ACh binding site carried by the α-subunits (Czajkowski and Karlin, 1991, 1995) and Asp180 and Glu189 of the δ-subunit (Czajkowski and Karlin, 1995). Based on these chemical data as well as on site-directed mutagenesis experiments (Czajkowski *et al.*, 1993), δAsp180 and δGlu189 may thus contribute to ligand binding (Czajkowski *et al.*, 1993) as part of the complementary component of the cholinergic ligand binding area (Galzi and Changeux, 1994; Corringer *et al.*, 1995; Karlin and Akabas, 1995). Interestingly, these two amino acids are respectively homologous to Asp163 and Glu172 of the α7 subunit (Figure 5C), and consistent with the data obtained on *Torpedo* receptor. Our study shows that mutations D163N and E172Q altogether alter ACh apparent affinity and calcium affinity. However, at variance to studies performed on *Torpedo* receptor, mutation of α7 Glu172 seems to affect ACh binding only as a consequence of calcium binding alterations.

The ACh and calcium sites which thus appear topographically distinct may be located in close proximity to each other and may even share amino acids from loop V. According to such a structural model, some functional groups from loop V, such as Glu172, would contribute to calcium binding, while others, such as Asp163, would contribute to ACh binding (Figure 5C). The tertiary and quaternary structural changes that take place in the course of receptor activation would then alter in a concerted manner the affinity of both sites for their respective ligands. Our data, in any case, open the way to an analysis of the metal ion binding sites which regulate the functional properties of the nicotinic receptors at loci distinct from the ion channel.

Materials and methods

Electrophysiological recordings

The α7-V201-$5HT_3$ (Eiselé *et al.*, 1993), the α7 receptor and their derived point mutants (Galzi *et al.*, 1992) were reconstituted in *Xenopus* oocytes and recorded as described in Bertrand *et al.* (1991). Current–voltage relationships were determined in the presence and absence of internal 1,2-bis(2-aminophenoxy)-ethane *N,N,N',N'*-tetraacetic acid (BAPTA) using ramps starting at negative and ending at positive potentials within 500 ms. On the α7-V201-$5HT_3$ receptor, calcium has no effect on reversal potentials in the presence of BAPTA. In the absence of BAPTA, a slight shift in reversal potential is observed (20 ± 7 mV, n = 3), which reflects weak calcium permeability and subsequent activation of the calcium-dependent chloride channels. Because of the ramp protocol, the ratio of *I–V* curves measured in the absence and presence of calcium is linear (in the presence of BAPTA), indicating no voltage-sensitive component of the effect of calcium on current amplitudes. Dose–response curve data are fitted using the simplex algorithm, and all curves (and curve ratios) are generated with the theoretical values given by the best fits.

Electrophysiological data analysis

Curve fitting of the agonist dose–response data point was performed using a sequential model (Del Castillo and Katz, 1957):

$$R + nF \overset{K}{\longleftrightarrow} RF \overset{K}{\longleftrightarrow} \ldots \overset{K}{\longleftrightarrow} RFn \overset{K_0}{\longleftrightarrow} OFn$$

where R are closed and O open channels, $K = ([R][F]^n)/[RFn]$ is the dissociation constant of the agonist for its n identical sites per receptor molecule, and $K_0 = [RFn]/[OFn]$ is the ratio of closed to open channels (Mulle *et al.*, 1992a).

The ionic response amplitude is given by $I = x/\{1 + [K_0\ (1 + K/F)^n]\}$, where x = (number of receptor molecules contributing to the response)×(unitary currents), F is the ligand concentration and n (the number of sites) is taken as five for both homooligomeric receptors (α7-V201-$5HT_3$ chimera and $5HT_3$) (Lindstrom, 1995; Palma *et al.*, 1996). Dose–response curves are fitted assuming that the same number of receptor molecules are activated in the absence and presence of calcium for the α7-V201-$5HT_3$ chimera and its mutants, and that for all wild-type and mutant $5HT_3$ receptors, channel block by calcium (2.5 mM) reduces the number of responsive receptor molecules to 35%. EC_{50} values are given by $EC_{50} = K/(\{[(2\times K_0 + 1)/K_0]^{1/n}\}-1)$ and Hill coefficients at EC_{50} are given by $nH = d\log([(I-I_{min})/(I_{max}-I_{min})]/\{1-[(I-I_{min})/(I_{max}-I_{min})]\})/d\log[F/M]$ with M = 1 mol/l.

The dissociation K and activation K_0 constants are adjusted pairwise and their ratios ($K_{[0.0Ca^{2+}]}/K_{[2.5Ca^{2+}]}$ and $K_{0[0.0Ca^{2+}]}/K_{0[2.5Ca^{2+}]}$), given in Table I, are indicative of alterations by calcium of binding or isomerization constants for activation.

Plots of I_{Ca}/I_{0Ca} versus agonist concentration report the ratios of

experimentally determined currents given in dose–response curves. The solid line is the ratio of the theoretical dose–response curves fitted for 0.0 and 2.5 mM Ca^{2+}.

As calcium is slightly permeable through the α7-V201-5HT_3 chimeric channel and subsequently activates calcium-dependent chloride channels, and because the extent of 5HT_3 channel block by calcium could not be estimated quantitatively for mutants 5HT_3 CA1 and 5HT_3 CA2, no further determination of intrinsic calcium affinity for its regulatory sites was attempted.

Dose–response curves were also adjusted with the two-state allosteric scheme (Monod *et al.*, 1965):

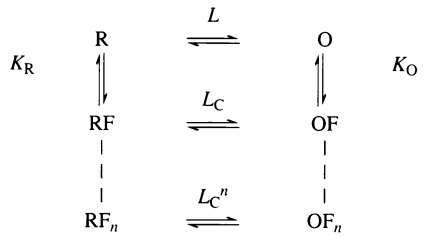

with the fraction of open channels $O = [(1 + \alpha)^n]/[(1 + \alpha)^n + {}^{RO}L(1 + {}^{RO}c\alpha)^n]$, where n is the number of sites, α is the concentration of ligand [F] normalized to its affinity for the *O* state ($\alpha = [F]/K_O$), ${}^{RO}c$ is the ratio of dissociation constants for the R and O states (${}^{RO}c = K_O/K_R$), and ${}^{RO}L$ is the equilibrium constant between the R and O states in the absence of added ligand (${}^{RO}L = [R]/[O]$). The fitting of α7-V201-5HT_3 chimera (and its loop V mutant's) dose–response curves in the absence and presence of calcium can be obtained with identical values for K_R, K_O and n, but with distinct ${}^{RO}L$ values (${}^{RO}L_{[0.0Ca^{2+}]}/{}^{RO}L_{[2.5Ca^{2+}]} = 20$ for α7-V201-5HT_3 in Figure 2A), in agreement with a nonexclusive binding of calcium (Rubin and Changeux, 1966).

Equilibrium binding

Equilibrium binding experiments were performed as described by Corringer *et al.* (1995). cDNAs were transfected into HEK 293 cells by calcium phosphate precipitation. [^{125}I]α-Bgtx binding measurements were performed at 18°C on intact cells. ACh apparent affinity (K_p value) was determined as the concentration reducing by 50% the initial velocity of 2.5 or 5.0 nM [^{125}I]α-Bgtx binding in the absence or presence of 10 mM calcium. The initial rate of [^{125}I]α-Bgtx binding was linear during the first 5 min of association at 2.5 or 5.0 nM. Although mutants D163N and D163A exhibited maximal ACh-evoked responses of similar magnitude when expressed in *Xenopus* oocytes, only mutant D163A exhibited α-Bgtx binding. The drastically reduced α-Bgtx binding capacity of mutant D163N may result from the occurrence of an NXS consensus glycosylation sequence. This issue has not been investigated further.

Fluorescence measurements

Fluorescence measurements were performed, as described in McManus *et al.* (1990), in 10 mM Tris–HCl buffer (pH 7.2) on a Perkin Elmer LS-5B spectrofluorimeter, with an excitation wavelength of 285 nm. Emission was monitored between 500 and 600 nm with a cut-off filter (Corning 3603-75C), and the peak centered at 545 nm was integrated for quantitation. Tb^{3+} at a fixed (10 μM) concentration is mixed with increasing concentrations of peptide. In the reverse experiment, where the peptide at a fixed concentration (10 μM) is mixed with increasing amounts of Tb^{3+}, energy transfer is also observed, but peptide precipitation occurs at Tb^{3+}:peptide ratios >1.5:1, precluding reliable titration.

Acknowledgements

We thank Drs S.Edelstein, H.Soldano and J.Haiech for discussions and C.Léna for critically reading the manuscript. This work was supported by grants from the Association Française contre les Myopathies, the Collège de France, the Centre National de la Recherche Scientifique, the Ministère de la Recherche, the Direction des Recherches Etudes et Techniques, the Human Frontier Science Program (to J.P.C.), The European Molecular Biology Organization (short-term fellowship to J.L.G.), the Swiss National Foundation, the OFES and the Human Frontier Science Program (to D.B.).

References

Amador,M. and Dani,J.A. (1995) *J. Neurosci.*, **15**, 4525–4532.
Assaf,S.Y. and Chung,S.H. (1984) *Nature*, **308**, 734–738.
Benninger,C., Kadis,J. and Prince,D.A. (1980) *Brain Res.*, **187**, 165–182.
Bertrand,D., Cooper,E., Valera,S., Rungger,D. and Ballivet,M. (1991) Electrophysiology of neuronal nicotinic acetylcholine receptors expressed in *Xenopus* oocytes, following nuclear injection of genes or cDNAs. In Conn,M. (ed.), *Methods in Neurosciences*. Academic Press Inc., New York, Vol. IV, pp. 174–193.
Bertrand,D., Galzi,J.L., Devillers-Thiéry,A., Bertrand,S. and Changeux, J.P. (1993) *Proc. Natl Acad. Sci. USA*, **90**, 6971–6975.
Brown,E.M., Vassilev,P.M. and Hebert,S.C. (1995) *Cell*, **83**, 679–682.
Chang,W.W. and Neumann,E. (1976) *Proc. Natl Acad. Sci. USA*, **73**, 3364–3368.
Cohen,J.B., Weber,M. and Changeux,J.P. (1974) *Mol. Pharmacol.*, **10**, 904–932.
Corringer,P.J., Galzi,J.L., Eiselé,J.L., Bertrand,S., Changeux,J.P. and Bertrand,D. (1995) *J. Biol. Chem.*, **270**, 11749–11752.
Couturier,S., Bertrand,D., Matter,J.M., Hernandez,M.C., Bertrand,S., Millar,N., Valera,S., Barkas,T. and Ballivet,M. (1990) *Neuron*, **5**, 845–856.
Czajkowski,C. and Karlin,A. (1991) *J. Biol. Chem.*, **266**, 22603–22612.
Czajkowski,C. and Karlin,A. (1995) *J. Biol. Chem.*, **270**, 3160–3164.
Czajkowski,C., Kaufman,C. and Karlin,A. (1993) *Proc. Natl Acad. Sci. USA*, **90**, 6285–6289.
Del Castillo,J. and Katz,B. (1957) *Proc. R. Soc. Lond.*, **146**, 339–356.
Draghun,A., Verdorn,T.A., Ewert,M. and Seeburg,P.H. (1990) *Neuron*, **5**, 781–788.
D'Souza,S.E., Haas,T.A., Piotrowitcz,R.S., Byers-Ward,V., McGrath, D.E., Soule,H.R., Cierniewski,C., Plow,E.F. and Smith,J.W. (1994) *Cell*, **79**, 659–667.
Eiselé,J.L., Bertrand,S., Galzi,J.L., Devillers-Thiéry,A., Changeux,J.P. and Bertrand,D. (1993) *Nature*, **366**, 479–483.
Fairclough,R.H., Miake-Lye,R.C., Stroud,R.M., Hodgson,K.O. and Doniach,S. (1986) *J. Mol. Biol.*, **189**, 673–680.
Falke,J.J., Drake,S.K., Hazard,A.L. and Peersen,O.B. (1994) *Quart. Rev. Biophys.*, **27**, 219–290.
Galzi,J.L. and Changeux,J.P. (1994) *Curr. Opin. Struct. Biol.*, **4**, 554–565.
Galzi,J.L., Devillers-Thiery,A., Hussy,N., Bertrand,S., Changeux,J.P. and Bertrand,D. (1992) *Nature*, **359**, 500–505.
Haiech,J. and Sallantin,J. (1985) *Biochimie*, **67**, 555–560.
Heidmann,T. and Changeux,J.P. (1979) *Eur. J. Biochem.*, **94**, 281–296.
Heinemann,U., Stabel,J. and Rausche,G. (1990) *Prog. Brain Res.*, **83**, 197–214.
Karlin,A. and Akabas,M. (1995) *Neuron*, **15**, 1231–1244.
Laube,B., Kuhse,J., Rundstrom,N., Kirsch,J., Schmeiden,V. and Betz,H. (1995) *J. Physiol.*, **483**, 613–619.
Léna,C. and Changeux,J.P. (1993) *Trends Neurosci.*, **16**, 181–186.
Lindstrom,J. (1995) In North,R.A. (ed.), *Handbook of Receptors and Channels*. CRC Press, New York, pp. 153–175.
Livsey,C.T., Huang,B., Xu,J. and Karwoski,C.J. (1990) *Vision Res.*, **6**, 853–861.
Maricq,A.V., Peterson,A.S., Brake,A.J., Myers,R.M. and Julius,D. (1991) *Science*, **254**, 432–437.
McDonald,R.L. and Olsen,R. (1994) *Annu. Rev. Neurosci.*, **17**, 569–602.
McManus,J.P., Hogue,C.W., Marsden,B., Sikorska,M. and Szabo,A.G. (1990) *J. Biol. Chem.*, **265**, 10358–10366.
Monod,J., Wyman,J. and Changeux,J.P. (1965) *J. Mol. Biol.*, **12**, 88–118.
Mulle,C., Léna,C. and Changeux,J.P. (1992a) *Neuron*, **8**, 937–945.
Mulle,C., Choquet,D., Korn,H. and Changeux,J.P. (1992b) *Neuron*, **8**, 135–143.
Palma,E., Bertrand,S., Binzoni,T. and Bertrand,D. (1996) *J. Physiol.*, **491**, 151–161.
Persechini,A., Moncrief,N.D. and Kretsinger,R.H. (1989) *Trends Neurosci.*, **12**, 462–467.
Pumain,R. and Heinemann,U. (1985) *J. Neurophysiol.*, **53**, 1–16.
Ramirez-Latorre,J.A. and Role,L. (1995) *Abstr. Soc. Neurosci.*, **21**, 527.3.
Rubin,M.M. and Changeux,J.P. (1966) *J. Mol. Biol.*, **21**, 265–274.
Rübsamen,H., Hess,G.P., Eldefrawi,A.T. and Eldefrawi,M.E. (1976a) *Biochem. Biophys. Res. Commun.*, **68**, 56–63.
Rübsamen,H., Montgomery,M., Hess,G.P., Eldefrawi,A.T. and Eldefrawi,M.E. (1976b) *Biochem. Biophys. Res. Commun.*, **70**, 1020–1026.
Rübsamen,H., Eldefrawi,A.T., Eldefrawi,M.E. and Hess,G.P. (1978) *Biochemistry*, **17**, 3818–3825.

Séguéla,P., Wadiche,J., Dineley-Miller,K., Dani,J.A. and Patrick,J.W. (1993) *J. Neurosci.*, **13**, 596–604.
Sine,S.M., Claudio,T. and Sigworth,F.J. (1990) *J. Gen. Physiol.*, **96**, 395–437.
Smart,T.G., Xie,X. and Krishek,B.J. (1994) *Prog. Neurobiol.*, **42**, 393–441.
Strynadka,N.C.J. and James,M.N.G. (1989) *Annu. Rev. Biochem.*, **58**, 851–898.
Vernino,S., Amador,M., Luetje,C.W., Patrick,J. and Dani,J.A. (1992) *Neuron*, **8**, 127–134.
Vernino,S., Rogers,M., Radcliffe,K.A. and Dani,J.A. (1994) *J. Neurosci.*, **14**, 5514–5524.
Weber,M. and Changeux,J.P. (1974) *Mol. Pharmacol.*, **10**, 1–14.

Received on May 2, 1996; revised on July 16, 1996